Utility of the Recombinase Driver CX3CR1::Cre Rat Strain to Evaluate Microglial Contributions to Nicotine Addiction

Ashley White[1], Ashley J. Craig[1], Daryl Richie[1], Christa L. Corley[1], Emma O. Bondy[1], Percell T. Kendrick, Jr., Michael D. Scofield[2], and Cassandra D. Gipson[1]*

[1]Department of Pharmacology and Nutritional Sciences, University of Kentucky, Lexington KY

[2]Department of Anesthesiology, Medical University of South Carolina, Charleston, SC

***Correspondence to:**

Cassandra D. Gipson, Ph.D.
Department of Pharmacology and Nutritional Sciences
University of Kentucky
900 S. Limestone
CTW Room 535
Lexington, KY, 40536, USA
Email: cdgips2@uky.edu
859-216-0625

Conflicts of interest: None
Funding Sources: This work was supported by the National Institutes of Health Grant DA058933, and DA055879, DA044479, DA046526, DA061626, and DA049130 (to CDG). All authors have no disclosures to declare.

Author Note: We would like to thank Mei Hong for technical assistance.

Abstract

Smoking remains a leading preventable cause of death, and nicotine is the primary substance responsible for maintaining use of tobacco products. Preclinical rodent models have shown that neuroimmune signaling is dysregulated by nicotine self-administration (SA) within the nucleus accumbens core (NAcore), which is a key region within the mesolimbic brain reward pathway. Microglia are the resident brain immune cell and prior studies have shown that they play an important role in nicotine-related behaviors. However, while there are transgenic mouse lines that allow for specific evaluations of microglia to neurobiology and behavior, there are fewer tools available for rats as a model species thus limiting our ability to evaluate specific contributions of microglia to nicotine SA. Using transgenic rats expressing Cre under the control of the CX3CR1 promoter bred on a Long Evans (LE) background, we show that NAcore microglia can be specifically transduced with Designer Receptors Exclusively Activated by Designer Drugs (DREADDs). We further show that CX3CR1::Cre rats readily self-administer nicotine, and display a characteristic extinction curve that is not different from outbred LE or Cre-negative littermates. Together, these validation studies lay the foundation for future use of this transgenic rat line to evaluate the specific contributions of microglia in the brain to neurobehavioral underpinnings of nicotine addiction.

-208 words-

KEYWORDS: Microglia, Nicotine, Self-administration, Behavior, DREADDs

45 **Introduction**

46 The immunomodulatory effects of nicotine have been clinically (Sher et al. 1999) and
47 preclinically (Li et al. 2021; Namba et al. 2019; Shi et al. 2009) documented, however, the
48 impacts of chronic, volitional nicotine use on neuroimmune signaling is a field in its infancy.
49 Microglia are resident brain immune cells which regulate adaptive and innate immune
50 responses (Paolicelli et al. 2022), regulate synaptic plasticity (Aramideh et al. 2021; Bessis et al.
51 2007; Paolicelli and Ferretti 2017), and are a part of the neurovascular unit (Liu et al. 2020).
52 Recent studies have implicated microglia in nicotine addiction processes as microglia within the
53 reward pathway and specifically the nucleus accumbens (NA) play a large role in regulating
54 nicotine-related neurobehavior (Kumar et al. 2024; Adeluyi et al. 2019; Soares and Picciotto
55 2024). However, our ability to specifically manipulate microglia to determine causal roles of
56 these brain immune cells in nicotine addiction processes remains limited.

57 The current neuroscience toolbox for evaluating microglia includes viruses, chemicals to
58 deplete them, and transgenic rodent models. Viruses that have been utilized in prior studies
59 include Designer Receptors Exclusively Activated by Designer Drugs (DREADDs) which
60 incorporate adeno-associated viral vectors (AAVs) with promoters that are thought to be
61 microglia-specific (e.g., CD68; (Grace et al. 2016), and AAV variants that allow *in vitro* and *in*
62 *vivo* microglial transduction through directed evolution of the AAV capsid protein to increase
63 efficiency of genetic payload into microglia (Lin et al. 2022). Notably, the pAAV-CD68-hM4D-
64 mCherry (Gi) and pAAV-CD68-EGFP DREADD utilized in (Grace et al. 2016) are commercially
65 available but untested in their ability to penetrate microglia within the brain as that study infused
66 DREADDs intrathecally. The AAV variants which were discovered a few years later to infect
67 microglia were also found to infect neurons (Lin et al. 2022), thus making it difficult to tease
68 apart microglial versus neuronal contributions to neurobiology and behavior.

69 As mentioned above, other methodologies to evaluate contributions of microglia to brain
70 function include depletion methodologies with either a Cx3cr1-Dtr rat, which allows for short-

71 term microglia depletion (De Luca et al. 2019), or with colony-stimulating factor–1 receptor
72 (CSF1R) inhibitors (e.g., PLX5622 or PLX3397), which deplete a proportion of microglia as well
73 as other affect peripheral cells (Green et al. 2020) when administered in chow. An advantage of
74 this technique is that microglia can repopulate (Wickel et al. 2024), allowing for bidirectional
75 evaluations of microglia to neurobiology and behavioral outcomes. However, microglia depletion
76 is non-specific and can have off target effects, limiting the cell-type specificity of this approach.
77 An additional methodology includes frequently utilized transgenic mouse strains which have
78 been used primarily in other fields of research. Transgenic mice, including the recombinase
79 driver CX3CR1-Cre strains (Zhao et al. 2019), have been used to visualize or manipulate
80 microglia in the context of other pathologies (Wieghofer and Prinz 2016). Endogenous CX3CR1
81 is a microglia-specific marker, and it is a receptor with the endogenous ligand fractalkine
82 (Nishiyori et al. 1998). However, there has been some debate regarding specificity of CX3CR1
83 to microglia, as there are reports that CX3CR1 expression occurs in other cell types depending
84 on the tissue type (Lee et al. 2018), or co-localization of CX3CR1 with glial fibrillary acidic
85 protein (GFAP; (Peng et al. 2017), a marker of astrocyte function (Middeldorp and Hol 2011),
86 although this has not been evaluated within the brain reward pathway to our knowledge. Some
87 studies have also reported that CX3CR1::cre in mice is not specific to microglia, with significant
88 leakage into neurons (Haimon et al. 2018; Hwang et al. 2017; Zhang et al. 2018). While there
89 are two constitutive and two tamoxifen-inducible CX3CR1::cre mouse lines (Gong et al. 2007;
90 Parkhurst et al. 2013; Yona et al. 2013), there is only one CX3CR1::cre rat line which has never
91 been utilized to evaluate microglia contributions to addiction neuroscience and has never been
92 demonstrated to allow for microglia-specific infection.
93 A large majority of studies modeling nicotine addiction utilize self-administration (SA), which
94 allows for evaluations of volitional nicotine use and is most frequently implemented in rat models
95 (Corley et al. 2024). Studies also frequently incorporate extinction training following SA to
96 evaluate the ability to learn to withhold the prepotent response to receive the drug and is

97 typically conducted under withdrawal conditions (Namba, et al., 2019). While some studies
98 incorporate mouse SA to model aspects of nicotine addiction (Fowler et al. 2011; Fowler and
99 Kenny 2011), use of mice in nicotine SA is limited to a small number of researchers and can
100 present challenges with catheter patency among other issues. While all currently available
101 methodologies to evaluate microglia have limitations with some noted above, the microglia
102 addiction field has a significant barrier in that there are no validated rat strains for use in SA
103 procedures. Here, we utilized a commercially available CX3CR1::cre transgenic rat strain (LE-
104 Tg(OTTC1005) CX3CR1-Cre-ERT2), which is a tamoxifen-inducible Cre recombinase strain
105 based on a Long Evans background. The goal of the current study was therefore to determine if
106 this rat strain (1) displays microglia-specific expression of viral vectors within the NAcore without
107 infecting surrounding neurons, and (2) can acquire nicotine SA and extinction (3) similar to
108 CX3CR1::cre (-) littermates and wildtype Long Evans rats.
109

110 **Methods**

111 Subjects.

112 Breeder male LE-Tg(OTTC1005) CX3CR1-Cre-ERT2 rats were purchased from the Rat
113 Resource and Research Center (RRRC) and bred in-house with Long Evans females purchased
114 from Charles River. Rats were housed in a temperature and humidity-controlled animal facility
115 within the Division of Laboratory Animal Resources (DLAR) at the University of Kentucky. The
116 colony room was on a 12:12 hr light:dark reverse light cycle and rats in the breeding colony had
117 *ad libitum* access to food and water. Rats in nicotine SA were either CX3CR1::Cre (+; N=50),
118 CX3CR1::Cre (-; N=15), or purchased from Charles River as an outbred strain control (N=37).
119 Male and female rats were 60-90 days old at the beginning of the study and were food restricted
120 to 85% of free feed weight throughout SA experimentation. All animal use practices were
121 approved by the Institutional Animal Care and Use Committee (IACUC) of the University of

122 Kentucky (UK; Protocol #2020-3438). 19 CX3CR1::Cre (+), 3 CX3CR1::Cre (-), and 2 Long Evans
123 rats were excluded from the study due to catheter patency issues.
124
125 CX3CR1::Cre Genotyping.
126 Ear punches were collected from all animals on post-natal day 21. In separate 1.5 mL
127 microcentrifuge tubes, ear punch tissues were incubated in lysis buffer and Proteinase K
128 (Invitrogen, ~2 mg/ml, 24 µl total volume) at 55°C for 30 minutes, vortexed, and pelleted (18,000
129 x g). Samples were incubated for an additional 30 min at 55°C, vortexed, then resuspended in
130 distilled water up to 200 µl total volume, and pelleted (18,000 x g). The samples were heated at
131 100°C for 10 minutes, cooled to room temperature, and pelleted at 18,000 x g for 20 minutes at
132 4°C. Next, 100 µl of the supernatant containing the genomic DNA was transferred to a new 1.5
133 ml microcentrifuge tube, and standard PCR amplification was used for genotyping.

134 Subjects were genotyped using the following primers: CX3CR1 F103289 (5'- TCAGGGTGG
135 CCCATAACCAC-3′) and CreETT2 R713 (5'-AGGTAGTTATTCGGATCATCAGCTTAC AC-3')
136 which produce a 1017 bp amplicon spanning the 5' end of the CX3CR1-Cre-ERT2. Primers
137 CX3CR1 F103289 (5'-TCAGGGTGGCCCATAACCAC-3′) and CREERT2 R246 (5'-CAGTGA
138 AGCTTCGATGATGGG C-3'), which produce a 550 bp amplicon spanning the 5' end of the
139 CX3CR1-Cre-ERT2. Primers CreERT2 F1206 (5'-CAGTGAAGCTTCGATGATGGGC-3') and
140 CX3CR1 R104157 – 5' – GCCAGATTTCCTGCAGGACCT- 3'), which produce a 1553 bp
141 amplicon spanning the 3' end of the CX3CR1-Cre-ERT2. All animals used were confirmed
142 CX3CR1::cre transgene-positive.

143 Surgical Procedures.
144 Rats included in the immunohistochemistry study underwent surgery for viral infusions
145 targeting the NAcore as previously described (Leyrer-Jackson et al. 2021). Rats included in the
146 nicotine SA study underwent jugular catheter surgery and virus infusion surgery. All rats were

147 anesthetized using ketamine hydrochloride (80–100 mg/kg, i.m.) and xylazine (8 mg/kg, i.m.) and
148 underwent surgical implantation of intravenous jugular catheters as well as stereotaxically infused
149 viral delivery within the NAcore. Intravenous jugular catheters (made from polyurethane tubing;
150 BTPU-040; Instech) were inserted 2.5–3 cm into the right jugular vein and were threaded
151 subcutaneously to the posterior side of the animal where it was connected to an indwelling back
152 port (Instech). Dental cement (SNAP or Ortho-Jet) was used to adhere the catheter to the port.
153 The indwelling port was sutured using 4–0 vicryl braided suture (Ethicons) subcutaneously ~2 cm
154 caudal from the shoulder blades. Following jugular vein catheterization, animals were immediately
155 transferred to a rat stereotaxic frame and NAcore guide cannulae were bilaterally aimed at the
156 NAcore according to a stereotaxic atlas (Paxinos and Watson 2007). Viral vectors encoding
157 DREADDs for microglia infection were infused into the NAcore of CX3Cr1::cre animals: pAAV-
158 EF1a-DIO-hM4D(Gi)-mCherry (inhibitory; titer: 1.2 × 1013 vg/ml; Addgene, #50461), pAAV-EF1a-
159 DIO-hM3D(Gq)-mCherry (excitatory; titer: 1.3 × 1013 vg/ml; Addgene, #50460; packaged into an
160 AAV5 vector by UNC Vector Core), or pAAV5-EF1a-DIO-mCherry (control; i.e., only mCherry-
161 expressing; titer: 1.5 × 1013 vg/ml; Addgene, #44362) at a volume of 0.5 µl per hemisphere. Ef1a
162 was selected as the promoter because it is abundantly expressed in all cell types (Wakabayashi-
163 Ito and Nagata 1994), it is double floxed, and both Gq and Gi coupled-versions are commercially
164 available. Rats were immediately administered cefazolin (100 mg/kg, i.v.) and heparin (10 U/ml,
165 i.v.) and for seven consecutive days during the recovery period. Meloxicam (1 mg/kg, i.v.) was
166 given immediately and for the first 3 d of the recovery period. For rats in the SA study, heparin (10
167 U/ml, i.v.) was administered daily. All rats received 4-hydroxytamoxifen (20 mg/kg, I.P.; (Hughes
168 et al. 2024) 3 weeks following virus infusion and 2 days prior to experimentation.
169

170 Food Training Procedures

171 All rats in the nicotine SA study (N = 30) underwent food training on the sixth day of
172 postoperative care. Food restriction to maintain 85% of free feed weight was implemented a

173 minimum of 2 h before food training initiation and was maintained for the duration of the
174 experiment. Food training sessions were 15 h duration, and one active lever press resulted in the
175 delivery of one food pellet [fixed-ratio-1 (FR1), schedule of reinforcement; Bio-Serv, 45 mg/pellet)
176 Concurrently, one food pellet was delivered every 20 min regardless of response. Light and tone
177 stimuli were not paired with pellet administration. Food training criteria was set to 2:1 active to
178 inactive lever presses throughout the session and a minimum of 200 active lever presses. Rats
179 that did not pass the initial food training session completed a second session before beginning
180 SA procedures (N=10). Rats unable to pass food training procedures were excluded from the
181 study (N = 8). All food training, SA, and extinction sessions were conducted in modular operant
182 conditioning chambers (13 ENV-008, 15 ENV-007; Med Associates), which have been previously
183 described in detail (Sadek et al. 2024; Maher et al. 2023; Leyrer-Jackson et al. 2021).
184
185 Nicotine SA Procedures.
186 Nicotine infusions (0.06 mg/kg/infusion) were paired with a compound stimulus
187 (light+tone) and was followed by a 20-s timeout period. Nicotine was delivered across a 5.9-s
188 duration, at a total volume of 0.1 ml of nicotine was administered per infusion. Infusions were
189 paired with cue lights, located above each lever, and a 2900-Hz tone was presented throughout
190 the duration of the nicotine infusion. Active lever presses during the timeout period were recorded,
191 but did not result in additional nicotine infusions. An inactive lever was extended at all times and
192 responses were recorded; however, presses yielded no programmed consequences or rewards.
193 Session duration was 2 h in length and a FR1 schedule of reinforcement was used. All animals
194 were required to complete a minimum of 10 sessions before moving into extinction with the
195 following criteria: ≥10 nicotine infusions obtained and ≥2:1 active/inactive lever press ratio.
196 Additionally, extinction is defined either by (1) the lack of delivery of a reinforcer that was
197 previously delivered after a response (e.g., responses on the active lever no longer result in
198 nicotine infusions), or (2) as the absence of a contingency between response and reinforcer (e.g.,

199 the nicotine infusion occurs regardless of an animals' response; see Rescorla and Skucy,
200 1969; Lattal and Lattal, 2012). Given that the reinforcer here (the nicotine infusion) is not delivered
201 following a time-out active lever press, the latter definition applies to these types of responses
202 and are therefore distinct from active lever presses that directly result in the initiation of a nicotine
203 infusion. Thus, these two types of lever presses were analyzed separately in the current study.

204 Following 10 non-consecutive criteria-making sessions, rats were moved to the extinction
205 phase which took place in the same boxes as self-administration. During the extinction phase,
206 active lever presses no longer resulted in nicotine infusions or associated cues. A minimum of 14
207 2-h extinction sessions was required for each animal. Extinction criteria were set at <30 active
208 lever presses on the last day of extinction. Eight animals were removed from the current study
209 because of not meeting self-administration criteria ($N = 5$) or lack of DREADD
210 expression/improper cannula placement ($N = 3$).

211 Immunohistochemistry.

212 Rats were anesthetized with an overdose of euthasol (excess of 0.25 ml/kg i.p.) and
213 transcardially perfused with 0.01 M PBS followed by 4% paraformaldehyde. Brains were then
214 coronally sliced on a vibratome at 60 μm for immunohistochemistry staining. All antibodies and
215 dilutions are listed in **Table 1**. To determine if the virus infected microglia cells in the NAcore,
216 NAcore sections were first incubated in anti-Iba-1 primary antibody that was diluted in 1% BSA,
217 0.3% Triton, .05% azide, and 0.01 M PBS for 24 hours at room temperature on a shaker. Sections
218 were then rinsed with 0.01 M PBS three times for 30 minutes each then incubated in a secondary
219 antibody conjugated to Alexa Fluor 488 for 2 hours. Sections were mounted onto glass slides and
220 coverslipped using an anti-fade mounting medium. Next, to determine if the virus infected
221 microglia that expressed the cre (+) genotype, NAcore sections were simultaneously stained with
222 2 primary antibodies (anti-Iba1, and anti-CX3CR1) that were diluted in 1% BSA, 0.3% Triton, .05%
223 azide, and 0.01 M PBS for 24 hours at room temperature on a shaker. Sections were then rinsed
224 and incubated in secondary antibodies conjugated to Alexa Fluor 488 and Alexa Fluor 594 for 2

225 hours. Sections were mounted onto glass slides and coverslipped using an anti-fade mounting
226 medium containing DAPI to visualize cell bodies. Next to show colocalization of infected microglia
227 without infected neurons, NACore sections were incubated in 2 primary antibodies (anti-Iba1, and
228 anti-NeuN) that were diluted in 1% BSA, 0.3% Triton, .05% azide, and 0.01 M PBS for 24 hours
229 at room temperature on a shaker. Sections were then rinsed and incubated in secondary
230 antibodies conjugated to Alexa Fluor 488 and Alexa Fluor 594 for 2 hours. All confocal
231 micrographs were captured using a Nikon A1R Inverted Confocal Microscope.

232 Statistical Analysis.

233 Food training lever press data, drug infusions, and lever press discrimination (active,
234 inactive) across sessions were analyzed using linear mixed effects (LME) modeling (JMP
235 software from SAS). Tukey's HSD was used as post-hoc pairwise comparisons on nominal
236 variables where appropriate ($\alpha = 0.05$). Subject was treated as a random factor and session
237 was treated as a continuous factor whereas group was evaluated as a nominal variable in all
238 relevant analyses. Model fits were conducted to determine the best model fit for the datasets
239 where appropriate, and the models with the lowest Akaike information criterion (AICc) were
240 selected. Lever discrimination was assessed as the ratio of active/active+inactive lever presses
241 (including infusion-earning and timeout active lever presses, as well as all inactive lever
242 presses).

243

244 **Results**

245 **Cre-Dependent Viruses Express Within NAcore Microglia**

246 Immunohistochemistry was first conducted to determine if the fluorescent mCherry tag
247 from the viruses expressed in NAcore microglia following intracranial viral delivery. Images were
248 taken using a Nikon A1R Confocal Microscope. **Figure 1A** shows that mCherry from the Gi viral
249 construct was successfully observed within NAcore Iba1-(+) cells. Similarly, we found co-
250 localization of mCherry with NAcore Iba1-(+) cells with the Gq construct (**Figure 1B**). To

251 determine specificity to CX3CR1-expressing cells, we next evaluated co-localization of mCherry
252 from the Gi construct with CX3CR1 and Iba-1. Notably, cells that were mCherry-(+) expressed
253 both microglia markers (**Figure 1C**), demonstrating that the CX3CR1::cre transgenic rat strain
254 allowed for AAV infection of microglia. Finally, we confirmed somatic expression of mCherry with
255 co-localization of the fluorescent tag with DAPI, which visualizes nuclear DNA (Tarnowski et al.
256 1991); **Figure 1D**). Next, we determined if mCherry from the Gi construct co-localized with the
257 neuronal marker NeuN. As shown in **Figure 1E**, there was no co-localization of mCherry with
258 NeuN, demonstrating specificity of mCherry to microglia within the NAcore.

259 **CX3CR1::cre Rats Acquire Nicotine SA and Extinction**

260 First, baseline nicotine consumption was compared during nicotine SA acquisition as a
261 function of virus groups following viral administration (see **Figure 2A** for an experimental timeline).
262 The best model fit excluded sex in the model (ΔAICc = 31.9, relative to the next best model fit,
263 which included both sex and group as a variable). LME revealed no significant main effects group
264 ($F_{2,2}$ = 0.6081, p>0.05), session ($F_{1,21}$ = 1.0336, p>0.05), or no group x session interactions ($F_{2,21}$
265 = 0.4445, p>0.05) (**Figure 3B**). These results indicate that virus administration did not change
266 nicotine SA acquisition rates regardless of the construct type. When nicotine consumption was
267 summed across experimentation, there were no group differences in the total amount of nicotine
268 consumption across the 15-day SA experiment ($F_{2,21}$ = 1.2943, p>0.05).

269 Next, data were collapsed across virus type and compared to CX3CR1::cre (-) littermates,
270 as well as purchased Long Evans rats. The best model fit excluded sex in the model (ΔAICc =
271 44.2, relative to the next best model fit, which included both sex and group as a variable). First
272 LME was conducted on lever discrimination during food training as a function of strain. No main
273 effect of strain ($F_{1,68}$ = 0.44, p>0.05 was found, indicating that all rats acquired food training
274 similarly with no strain differences in this effect. Baseline nicotine consumption was compared
275 during nicotine SA acquisition as a function of strain groups (see **Figure 3A** for an experimental
276 timeline). LME revealed no significant main effects of group ($F_{2, 64}$ = 1.1342, p>0.05), or session

277 ($F_{1, 64}$ = 3.0377, p>0.05) or group x session interactions ($F_{2, 64}$ = 2.2673, p>0.05) (**Figure 3B**).
278 These results indicate that the strain did not change nicotine SA acquisition rates regardless of
279 the genetic strain used. LME was conducted on lever discrimination during nicotine acquisition as
280 a function of strain. A significant main effect of strain ($F_{2,64.02}$ = 5.3284, p<0.05) was found,
281 however, all groups met the 2:1 active to inactive lever pressing ratio. When nicotine consumption
282 was summed across experimentation, there were no group ($F_{2,77}$ = 1.7039, p>0.05) differences in
283 the total amount of nicotine consumption across the 10-day SA experiment.
284
285 **Discussion**
286 Here we show that the CX3CR1::cre transgenic rat strain can be used to specifically
287 transduce DREADDs in microglia within a key region of the brain reward pathway, the NAcore,
288 and these rats can acquire intravenous nicotine SA and also undergo successful nicotine
289 extinction training. We compared acquisition curves across virus type and across strain with no
290 differences in either analyses. As noted previously, evaluations of microglia in addiction
291 neurobiology have been limited due to the tools available to study this cell type in rat models. Our
292 current data reported here support the use of this transgenic rat strain in the addiction
293 neuroscience field to evaluate microglia contributions to substance use, and particularly, in the
294 nicotine addiction field.
295 While the current study demonstrates the utility of this rat strain for studying aspects of
296 addiction neuroscience, there are notable limitations that must be outlined. It is important to note
297 that the current study did not functionally evaluate the impacts of chemogenetic activation or
298 inhibition on NAcore microglia, including evaluations of transcriptomic, epigenetic, metabolomic,
299 or proteomic changes induced by activation of the DREADD receptors. This is important because
300 the microglia field has recently shifted from a dichotomous thinking of “activated” versus “resting”
301 microglial states to a more complex multidimensional approach to microglial states (Paolicelli et
302 al. 2022). It is also unknown how muscarinic DREADD receptors expressed on CX3CR1(+)

303 microglia may shift these dynamic aspects of these immune cells. One study did find that
304 activation of Gi DREADDs expressed in microglia of CX3CR1$^{creER/+}$:R26$^{LSL\text{-}hM4Di/+}$ transgenic mice
305 inhibited chronic pain and spinal nerve transection-induced microglial reactivity (Yi et al. 2021).
306 This study also found that the Gi DREADD reduced interferon regulatory factor 8 (IRF8) and
307 interleukin (IL)-1β expression in Iba1(+) cells, although this study did not confirm that all microglia
308 were DREADD(+). Further, while this rat strain allows for infection of CX3CR1(+) microglia, this
309 methodology requires these cells to be virally infected with the construct. Here we did not find that
310 all microglia within the NAcore were mCherry(+), indicating that some microglia within the area of
311 viral delivery were not infected with the constructs. This could either be due to (1) too little infused
312 volume of the virus to perfuse through the visualized area of the NAcore, (2) some microglia did
313 not express cre, or (3) some microglia were able to mount an immune response from the viral
314 constructs. It is also important to note that this rat strain requires tamoxifen injections. Given that
315 tamoxifen is a selective estrogen receptor modulator and may have sex-specific antiestrogenic
316 effects (Rochefort and Borgna 1981) that could interfere with experimental outcomes, future
317 studies incorporating CX3CR1::cre rats should take this into account in experimental timelines.
318 Here, rats were administered tamoxifen several weeks prior to quantification of microglia
319 morphology, and during the early part of nicotine SA acquisition. Importantly, tamoxifen has a
320 half-life of 10.3 hrs in rats (Robinson et al. 1991), and five elimination half-lives are required for
321 approximately 97% of the bioavailable dose of a drug to be eliminated from the body (here, 51.5
322 hrs would be required; (Nnane 2005). Given this and that no sex differences were found in the
323 nicotine SA acquisition curves, it is unlikely that tamoxifen impacted behavioral outcomes here.
324 As well, another study administered 4-OHT immediately prior to cocaine conditioning and
325 observed measurable cocaine place preference in mice (Hughes et al. 2024). Finally, it is not
326 clear if CX3CR1::cre rat line has altered constitutive CX3CL1/CX3CR1 signaling, which is
327 important in neuron/microglia crosstalk in brain injury and inflammation (Pawelec et al. 2020).
328 Despite these caveats, this rat strain may allow for more granular *in vivo* evaluations of microglia

329 to glutamate dyshomeostasis induced by addictive drugs (Scofield et al. 2016) including nicotine
330 (Gipson et al. 2013), as well as cell type-specific dissections of glial contributions to the
331 neurobehavior of nicotine addiction.

332 **Conclusions**

333 Here, we have shown that the inducible recombinase driver CX3CR1::Cre rat strain can
334 be successfully used in a model of nicotine SA. CX3CR1::Cre rats readily self-administer nicotine,
335 while the viral constructs successfully infected microglia without neuronal co-infection within the
336 NAcore, eliminating one of the main issues with other methodologies utilizing viral constructs.
337 While mouse nicotine SA can be conducted successfully (Souter, et al., 2022), the majority of SA
338 studies utilize rats as the model rodent species, thus this rat will provide researchers with the
339 toolbox to readily manipulate microglia in rats undergoing SA of addictive drugs. Understanding
340 these contributions will provide insights on the neuroimmune landscape of nicotine addiction and
341 how immune modulation in different areas of the brain affect behavior.

342

343 -- 3854 words --

344

345

346 **Table 1. Antibodies for Immunohistochemistry**
347

Target	Company	Catalogue #	RRID	Dilution
Mouse Anti-NeuN antibody	Abcam	ab104224	RRID:AB_10711040	1:500
AlexaFluor 488 goat anti-chicken IgY	Abcam	ab150173	RRID:AB_2636995	1:500
Anti Iba1, Rabbit	Fujifilm	019-19741	RRID:AB_839504	1:500
Anti CX3CR1, Mouse	Abcam	ab167571	RRID:AB_2916288	1:500
DAPI antibody	Thermo Fisher	D1306	RRID:AB_2629482	1:1000

348

349 **Figure Legends.**

350 **Figure 1. NAcore Microglia but not Neurons Are Transduced with AAV Constructs.**
351 Representative immunohistochemical images from animals receiving viral infusions are shown.
352 Slices were stained with either whole cell microglial marker, Iba1; Cre-recombinase marker,
353 mCherry; microglial receptor, CX3CR1; cell soma marker, DAPI, and/or neuronal cell marker,
354 NeuN. Merged images show overlap of microglial and viral markers, indicating infection of
355 microglia with viral constructs without neuronal infection. AC = anterior commissure, denoted by
356 a dotted line.

357

358 **Figure 2. CX3CR1::cre Rats Acquire Nicotine SA and Extinction.** (A) Experimental timeline
359 for CX3CR1::cre rats. (B) Food training where animals met a 2:1 active to inactive lever
360 pressing ratio compared across virus groups with no significant differences *($p>0.05$)*. (C_{1-2})
361 CX3CR1::cre rats acquired lever responding to the active lever to receive IV infusions of
362 nicotine (0.06mg/kg/infusion) with no differences in lever discrimination. (D) CX3CR1::cre rats
363 had no significant differences in total nicotine consumption across the 15 day timeline. (E)
364 CX3CR1::cre rats showed a decline in lever pressing behavior during extinction training to < 30
365 lever presses per session.

366

367 **Figure 3. CX3CR1::cre Rats Acquire Nicotine SA similarly to Cre-negative Littermates and**
368 **Wild-Type rats.** (A) Experimental timeline for cre-negative littermates and ordered wild-type
369 rats from Charles River. (B) Food training where animals met a 2:1 active to inactive lever
370 pressing ratio compared across strain groups with no significant differences *($p>0.05$)*. (C) Rats
371 had no significant differences in total nicotine consumption across the 10 day timeline across
372 strains. (D_{1-2}) CX3CR1::cre rats acquired lever responding to the active lever to receive IV
373 infusions of nicotine (0.06mg/kg/infusion) compared to cre-negative littermates and wild-type
374 ordered animals with a significant difference in lever discrimination between strains ($p<0.05$).

375

376 **Figure 1.**
377

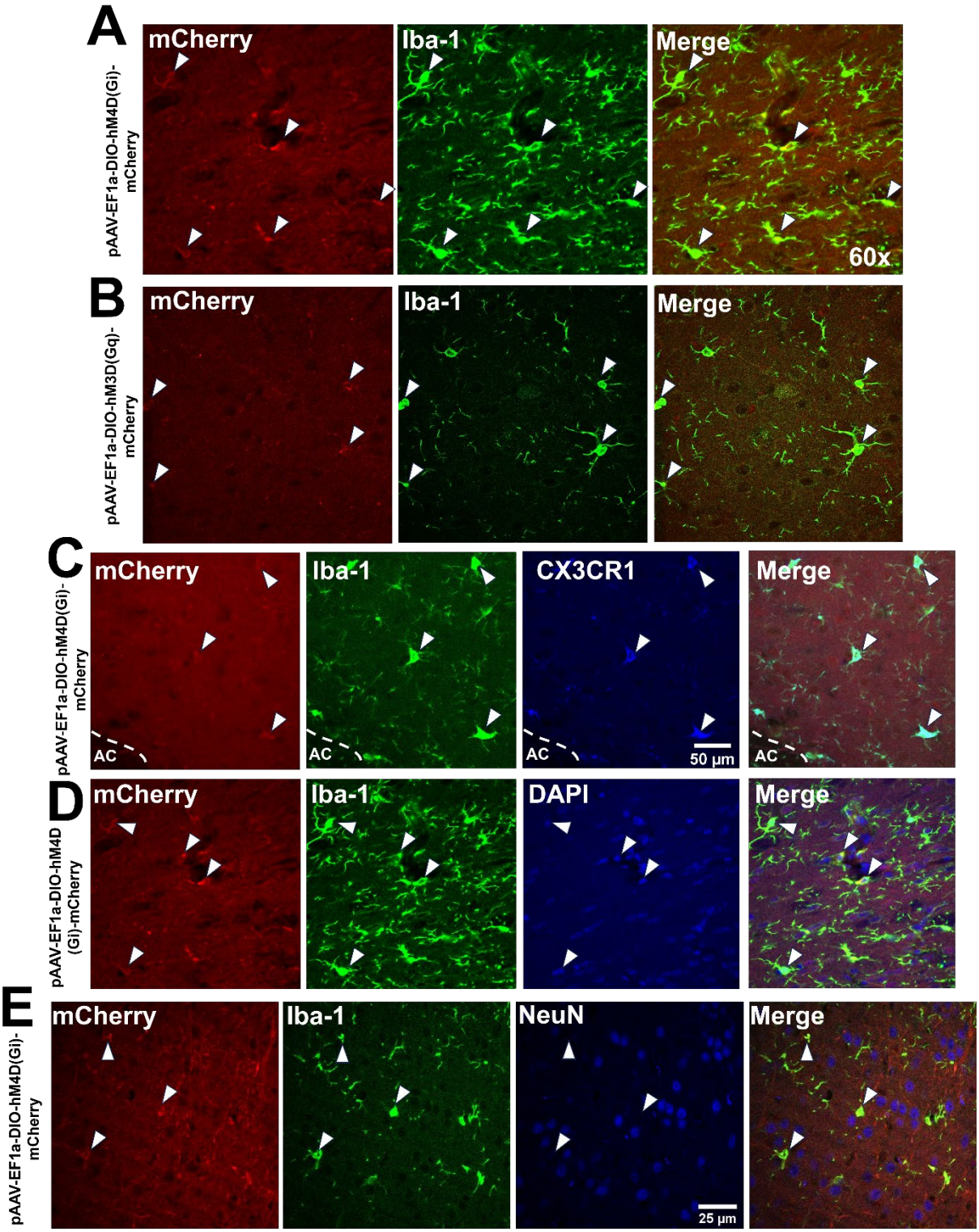

378 **Figure 2.**

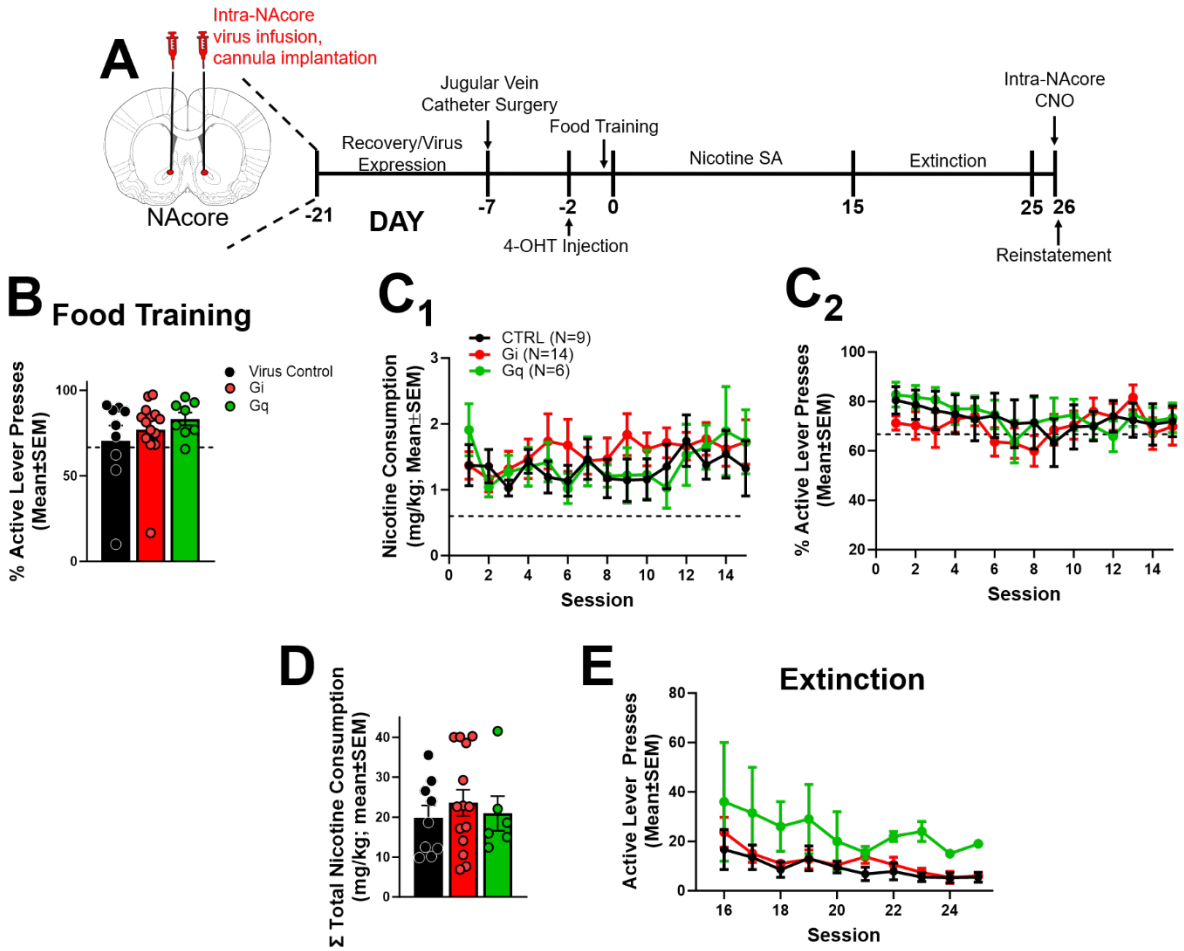

379

380

381

382

383

384 **Figure 3.**

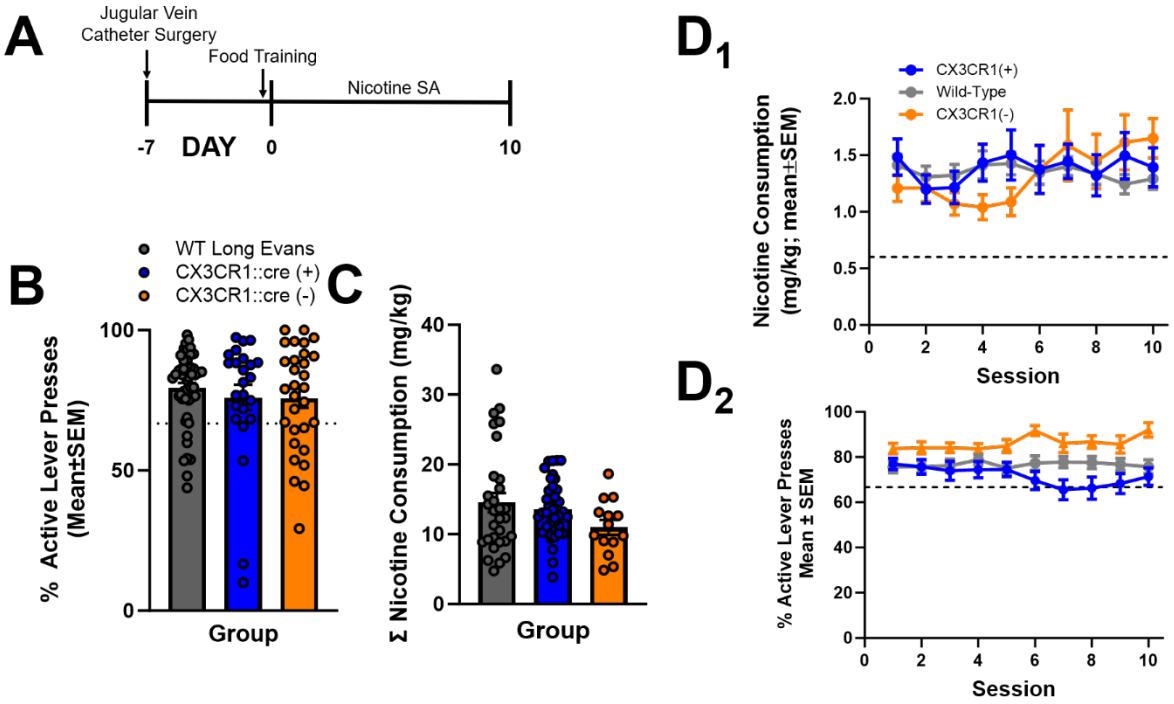

385

386

387

REFERENCES

Adeluyi A, Guerin L, Fisher ML, Galloway A, Cole RD, Chan SSL, Wyatt MD, Davis SW, Freeman LR, Ortinski PI, Turner JR (2019) Microglia morphology and proinflammatory signaling in the nucleus accumbens during nicotine withdrawal. Sci Adv 5 (10):eaax7031. doi:10.1126/sciadv.aax7031

Aramideh JA, Vidal-Itriago A, Morsch M, Graeber MB (2021) Cytokine Signalling at the Microglial Penta-Partite Synapse. Int J Mol Sci 22 (24). doi:10.3390/ijms222413186

Bessis A, Bechade C, Bernard D, Roumier A (2007) Microglial control of neuronal death and synaptic properties. Glia 55 (3):233-238. doi:10.1002/glia.20459

Corley C, Craig A, Sadek S, Marusich JA, Chehimi SN, White AM, Holdiness LJ, Reiner BC, Gipson CD (2024) Enhancing translation: A need to leverage complex preclinical models of addictive drugs to accelerate substance use treatment options. Pharmacol Biochem Behav 243:173836. doi:10.1016/j.pbb.2024.173836

De Luca SN, Sominsky L, Soch A, Wang H, Ziko I, Rank MM, Spencer SJ (2019) Conditional microglial depletion in rats leads to reversible anorexia and weight loss by disrupting gustatory circuitry. Brain Behav Immun 77:77-91. doi:10.1016/j.bbi.2018.12.008

Fowler CD, Kenny PJ (2011) Intravenous nicotine self-administration and cue-induced reinstatement in mice: Effects of nicotine dose, rate of drug infusion and prior instrumental training. Neuropharmacology 61 (4):687-698. doi:10.1016/j.neuropharm.2011.05.012

Fowler CD, Lu Q, Johnson PM, Marks MJ, Kenny PJ (2011) Habenular alpha5 nicotinic receptor subunit signalling controls nicotine intake. Nature 471 (7340):597-601. doi:10.1038/nature09797

Gipson CD, Reissner KJ, Kupchik YM, Smith AC, Stankeviciute N, Hensley-Simon ME, Kalivas PW (2013) Reinstatement of nicotine seeking is mediated by glutamatergic plasticity. Proc Natl Acad Sci U S A 110 (22):9124-9129. doi:10.1073/pnas.1220591110

Gong S, Doughty M, Harbaugh CR, Cummins A, Hatten ME, Heintz N, Gerfen CR (2007) Targeting Cre recombinase to specific neuron populations with bacterial artificial chromosome constructs. J Neurosci 27 (37):9817-9823. doi:10.1523/jneurosci.2707-07.2007

Grace PM, Strand KA, Galer EL, Urban DJ, Wang X, Baratta MV, Fabisiak TJ, Anderson ND, Cheng K, Greene LI, Berkelhammer D, Zhang Y, Ellis AL, Yin HH, Campeau S, Rice KC, Roth BL, Maier SF, Watkins LR (2016) Morphine paradoxically prolongs neuropathic pain in rats by amplifying spinal NLRP3 inflammasome activation. Proc Natl Acad Sci U S A 113 (24):E3441-3450. doi:10.1073/pnas.1602070113

Green KN, Crapser JD, Hohsfield LA (2020) To Kill a Microglia: A Case for CSF1R Inhibitors. Trends Immunol 41 (9):771-784. doi:10.1016/j.it.2020.07.001

Haimon Z, Volaski A, Orthgiess J, Boura-Halfon S, Varol D, Shemer A, Yona S, Zuckerman B, David E, Chappell-Maor L, Bechmann I, Gericke M, Ulitsky I, Jung S (2018) Re-evaluating microglia expression profiles using RiboTag and cell isolation strategies. Nat Immunol 19 (6):636-644. doi:10.1038/s41590-018-0110-6

Hughes BW, Huebschman JL, Tsvetkov E, Siemsen BM, Snyder KK, Akiki RM, Wood DJ, Penrod RD, Scofield MD, Berto S, Taniguchi M, Cowan CW (2024) NPAS4 supports cocaine-conditioned cues in rodents by controlling the cell type-specific activation balance in the nucleus accumbens. Nature communications 15 (1):5971. doi:10.1038/s41467-024-50099-1

Hwang HW, Saito Y, Park CY, Blachère NE, Tajima Y, Fak JJ, Zucker-Scharff I, Darnell RB (2017) cTag-PAPERCLIP Reveals Alternative Polyadenylation Promotes Cell-Type Specific Protein Diversity and Shifts Araf Isoforms with Microglia Activation. Neuron 95 (6):1334-1349.e1335. doi:10.1016/j.neuron.2017.08.024

438 Kumar M, Keady J, Aryal SP, Hessing M, Richards CI, Turner JR (2024) The Role of Microglia
439 in Sex- and Region-Specific Blood-Brain Barrier Integrity During Nicotine Withdrawal.
440 Biol Psychiatry Glob Open Sci 4 (1):182-193. doi:10.1016/j.bpsgos.2023.08.019
441 Lee M, Lee Y, Song J, Lee J, Chang SY (2018) Tissue-specific Role of CX(3)CR1 Expressing
442 Immune Cells and Their Relationships with Human Disease. Immune Netw 18 (1):e5.
443 doi:10.4110/in.2018.18.e5
444 Leyrer-Jackson JM, Holter M, Overby PF, Newbern JM, Scofield MD, Olive MF, Gipson CD
445 (2021) Accumbens Cholinergic Interneurons Mediate Cue-Induced Nicotine Seeking and
446 Associated Glutamatergic Plasticity. eNeuro 8 (1). doi:10.1523/ENEURO.0276-20.2020
447 Li H, Peng Y, Lin C, Zhang X, Zhang T, Wang Y, Li Y, Wu S, Wang H, Hutchinson MR, Watkins
448 LR, Wang X (2021) Nicotine and its metabolite cotinine target MD2 and inhibit TLR4
449 signaling. Innovation (Camb) 2 (2):100111. doi:10.1016/j.xinn.2021.100111
450 Lin R, Zhou Y, Yan T, Wang R, Li H, Wu Z, Zhang X, Zhou X, Zhao F, Zhang L, Li Y, Luo M
451 (2022) Directed evolution of adeno-associated virus for efficient gene delivery to
452 microglia. Nat Methods 19 (8):976-985. doi:10.1038/s41592-022-01547-7
453 Liu LR, Liu JC, Bao JS, Bai QQ, Wang GQ (2020) Interaction of Microglia and Astrocytes in the
454 Neurovascular Unit. Front Immunol 11:1024. doi:10.3389/fimmu.2020.01024
455 Maher EE, White AM, Craig A, Khatri S, Kendrick PT, Jr., Matocha ME, Bondy EO, Pallem N,
456 Breakfield G, Botkins M, Sweatt O, Griffin WC, Kaplan B, Weafer JJ, Beckmann JS,
457 Gipson CD (2023) Synthetic contraceptive hormones occlude the ability of nicotine to
458 reduce ethanol consumption in ovary-intact female rats. Drug Alcohol Depend
459 252:110983. doi:10.1016/j.drugalcdep.2023.110983
460 Middeldorp J, Hol EM (2011) GFAP in health and disease. Prog Neurobiol 93 (3):421-443.
461 doi:10.1016/j.pneurobio.2011.01.005
462 Namba MD, Kupchik YM, Spencer SM, Garcia-Keller C, Goenaga JG, Powell GL, Vicino IA,
463 Hogue IB, Gipson CD (2019) Accumbens neuroimmune signaling and dysregulation of
464 astrocytic glutamate transport underlie conditioned nicotine-seeking behavior. Addict
465 Biol:e12797. doi:10.1111/adb.12797
466 Nishiyori A, Minami M, Ohtani Y, Takami S, Yamamoto J, Kawaguchi N, Kume T, Akaike A,
467 Satoh M (1998) Localization of fractalkine and CX3CR1 mRNAs in rat brain: does
468 fractalkine play a role in signaling from neuron to microglia? FEBS Lett 429 (2):167-172.
469 doi:10.1016/s0014-5793(98)00583-3
470 Nnane IP (2005) PHARMACOKINETICS: Absorption, Distribution, and Elimination. In: Paul
471 Worsfold AT, Colin Poole (ed) Encyclopedia of Analytical Science. 2nd edn. Elsevier, pp
472 126-133. doi:https://doi.org/10.1016/B0-12-369397-7/00458-1.
473 Paolicelli RC, Ferretti MT (2017) Function and Dysfunction of Microglia during Brain
474 Development: Consequences for Synapses and Neural Circuits. Front Synaptic Neurosci
475 9:9. doi:10.3389/fnsyn.2017.00009
476 Paolicelli RC, Sierra A, Stevens B, Tremblay ME, Aguzzi A, Ajami B, Amit I, Audinat E,
477 Bechmann I, Bennett M, Bennett F, Bessis A, Biber K, Bilbo S, Blurton-Jones M,
478 Boddeke E, Brites D, Brône B, Brown GC, Butovsky O, Carson MJ, Castellano B,
479 Colonna M, Cowley SA, Cunningham C, Davalos D, De Jager PL, de Strooper B, Denes
480 A, Eggen BJL, Eyo U, Galea E, Garel S, Ginhoux F, Glass CK, Gokce O, Gomez-Nicola
481 D, González B, Gordon S, Graeber MB, Greenhalgh AD, Gressens P, Greter M,
482 Gutmann DH, Haass C, Heneka MT, Heppner FL, Hong S, Hume DA, Jung S,
483 Kettenmann H, Kipnis J, Koyama R, Lemke G, Lynch M, Majewska A, Malcangio M,
484 Malm T, Mancuso R, Masuda T, Matteoli M, McColl BW, Miron VE, Molofsky AV, Monje
485 M, Mracsko E, Nadjar A, Neher JJ, Neniskyte U, Neumann H, Noda M, Peng B, Peri F,
486 Perry VH, Popovich PG, Pridans C, Priller J, Prinz M, Ragozzino D, Ransohoff RM,
487 Salter MW, Schaefer A, Schafer DP, Schwartz M, Simons M, Smith CJ, Streit WJ, Tay
488 TL, Tsai LH, Verkhratsky A, von Bernhardi R, Wake H, Wittamer V, Wolf SA, Wu LJ,

Wyss-Coray T (2022) Microglia states and nomenclature: A field at its crossroads. Neuron 110 (21):3458-3483. doi:10.1016/j.neuron.2022.10.020

Parkhurst CN, Yang G, Ninan I, Savas JN, Yates JR, 3rd, Lafaille JJ, Hempstead BL, Littman DR, Gan WB (2013) Microglia promote learning-dependent synapse formation through brain-derived neurotrophic factor. Cell 155 (7):1596-1609. doi:10.1016/j.cell.2013.11.030

Pawelec P, Ziemka-Nalecz M, Sypecka J, Zalewska T (2020) The Impact of the CX3CL1/CX3CR1 Axis in Neurological Disorders. Cells 9 (10). doi:10.3390/cells9102277

Paxinos G, Watson C (2007) The rat brain in stereotaxic coordinates. 6th edn. Academic Press/Elsevier, Amsterdam ; Boston ;

Peng Y, Guo G, Shu B, Liu D, Su P, Zhang X, Gao F (2017) Spinal CX3CL1/CX3CR1 May Not Directly Participate in the Development of Morphine Tolerance in Rats. Neurochem Res 42 (11):3254-3267. doi:10.1007/s11064-017-2364-z

Robinson SP, Langan-Fahey SM, Johnson DA, Jordan VC (1991) Metabolites, pharmacodynamics, and pharmacokinetics of tamoxifen in rats and mice compared to the breast cancer patient. Drug Metab Dispos 19 (1):36-43

Rochefort H, Borgna JL (1981) Differences between oestrogen receptor activation by oestrogen and antioestrogen. Nature 292 (5820):257-259. doi:10.1038/292257a0

Sadek SM, Khatri SN, Kipp Z, Dunn KE, Beckmann JS, Stoops WW, Hinds TD, Jr., Gipson CD (2024) Impacts of xylazine on fentanyl demand, body weight, and acute withdrawal in rats: A comparison to lofexidine. Neuropharmacology 245:109816. doi:10.1016/j.neuropharm.2023.109816

Scofield MD, Heinsbroek JA, Gipson CD, Kupchik YM, Spencer S, Smith AC, Roberts-Wolfe D, Kalivas PW (2016) The Nucleus Accumbens: Mechanisms of Addiction across Drug Classes Reflect the Importance of Glutamate Homeostasis. Pharmacol Rev 68 (3):816-871. doi:10.1124/pr.116.012484

Sher ME, Bank S, Greenberg R, Sardinha TC, Weissman S, Bailey B, Gilliland R, Wexner SD (1999) The influence of cigarette smoking on cytokine levels in patients with inflammatory bowel disease. Inflamm Bowel Dis 5 (2):73-78. doi:10.1097/00054725-199905000-00001

Shi FD, Piao WH, Kuo YP, Campagnolo DI, Vollmer TL, Lukas RJ (2009) Nicotinic attenuation of central nervous system inflammation and autoimmunity. J Immunol 182 (3):1730-1739. doi:10.4049/jimmunol.182.3.1730

Soares AR, Picciotto MR (2024) Nicotinic regulation of microglia: potential contributions to addiction. J Neural Transm (Vienna) 131 (5):425-435. doi:10.1007/s00702-023-02703-94

Souter, E. A., Chen, Y. C., Zell, V., Lallai, V., Steinkellner, T., Conrad, W. S., Wisden, W., Harris, K. D., Fowler, C. D., & Hnasko, T. S. (2022). Disruption of VGLUT1 in Cholinergic Medial Habenula Projections Increases Nicotine Self-Administration. eNeuro, 9(1), ENEURO.0481-21.2021. https://doi.org/10.1523/ENEURO.0481-21.2021

Tarnowski BI, Spinale FG, Nicholson JH (1991) DAPI as a useful stain for nuclear quantitation. Biotech Histochem 66 (6):297-302

Wakabayashi-Ito N, Nagata S (1994) Characterization of the regulatory elements in the promoter of the human elongation factor-1 alpha gene. J Biol Chem 269 (47):29831-29837

Wickel J, Chung HY, Ceanga M, von Stackelberg N, Hahn N, Candemir Ö, Baade-Büttner C, Mein N, Tomasini P, Woldeyesus DM, Andreas N, Baumgarten P, Koch P, Groth M, Wang ZQ, Geis C (2024) Repopulated microglia after pharmacological depletion decrease dendritic spine density in adult mouse brain. Glia 72 (8):1484-1500. doi:10.1002/glia.24541

Wieghofer P, Prinz M (2016) Genetic manipulation of microglia during brain development and disease. Biochim Biophys Acta 1862 (3):299-309. doi:10.1016/j.bbadis.2015.09.019

540 Yi MH, Liu YU, Liu K, Chen T, Bosco DB, Zheng J, Xie M, Zhou L, Qu W, Wu LJ (2021)
541 Chemogenetic manipulation of microglia inhibits neuroinflammation and neuropathic
542 pain in mice. Brain Behav Immun 92:78-89. doi:10.1016/j.bbi.2020.11.030
543 Yona S, Kim KW, Wolf Y, Mildner A, Varol D, Breker M, Strauss-Ayali D, Viukov S, Guilliams M,
544 Misharin A, Hume DA, Perlman H, Malissen B, Zelzer E, Jung S (2013) Fate mapping
545 reveals origins and dynamics of monocytes and tissue macrophages under
546 homeostasis. Immunity 38 (1):79-91. doi:10.1016/j.immuni.2012.12.001
547 Zhang B, Zou J, Han L, Beeler B, Friedman JL, Griffin E, Piao YS, Rensing NR, Wong M (2018)
548 The specificity and role of microglia in epileptogenesis in mouse models of tuberous
549 sclerosis complex. Epilepsia 59 (9):1796-1806. doi:10.1111/epi.14526
550 Zhao XF, Alam MM, Liao Y, Huang T, Mathur R, Zhu X, Huang Y (2019) Targeting Microglia
551 Using Cx3cr1-Cre Lines: Revisiting the Specificity. eNeuro 6 (4).
552 doi:10.1523/ENEURO.0114-19.2019

553